

**SYSTEM-LEVEL MODELING OF COOLING  
NETWORKS IN ALL ELECTRIC  
SHIPS**

H. Babae

**MITSG 14-18**

Sea Grant College Program  
Massachusetts Institute of Technology  
Cambridge, Massachusetts 02139

NOAA Grant No. N000141410166

Project No. 2012-ESRDC-02-LEV

# System-level Modeling of Cooling Networks in All Electric Ships

**Hessam Babae**

*MIT Sea Grant, Massachusetts Institute of Technology*

# Contents

<b>1</b>	<b>Problem Description</b>	<b>3</b>
1.1	Task 3.2.1 . . . . .	3
<b>2</b>	<b>Summary of Accomplishments</b>	<b>3</b>
<b>3</b>	<b>Task 3.2.1 System-Level Thermal Modeling</b>	<b>4</b>
3.1	Development of 1D Transient Flow Model (MIT) . . . . .	4
3.1.1	Modeling Assumptions . . . . .	4
3.1.2	Mathematical Modeling . . . . .	4
3.2	Development of 1D Transient Heat Transfer Model (MIT) . . . . .	5
3.2.1	Modeling Assumptions . . . . .	5
3.2.2	Mathematical Modeling . . . . .	5
3.3	Component Modeling . . . . .	8
3.3.1	Pump . . . . .	8
3.3.2	Bend . . . . .	9
3.3.3	Valve . . . . .	10
3.3.4	Heat Exchanger . . . . .	10
3.4	Numerical Method . . . . .	11
3.5	Coupling of $\mathcal{N}\epsilon\kappa\tau\alpha r1d$ and vemESRDC: Collaboration between MIT and FSU .	12
3.6	Verification and Validation (MIT) . . . . .	13
3.6.1	A Single Loop with a Pump . . . . .	13
3.6.2	$\mathcal{N}\epsilon\kappa\tau\alpha r1d$ -vemESRDC Coupling (MIT-FSU) . . . . .	17
<b>4</b>	<b>Conclusion and Future Work</b>	<b>22</b>

## Abstract

*A Thermal management simulation tool is required to rapidly and accurately evaluate and mitigate the adverse effects of increased heat loads in the initial stages of design in all electric ships. By reducing the dimension of Navier-Stokes and energy equations, we have developed one-dimensional partial differential equations models that simulate time-dependent hydrodynamics and heat transport in a piping network system. Beside the steady-state response, the computational model enables us to predict the transient behavior of the cooling system, when the operating conditions are time-variant. To accurately predict the impact of cooling system on temperature distribution at different ship's locations/components and vice versa, we coupled our computational tool with vemESRDC developed at Florida State University. We verified our implementation with several benchmark problems.*

## 1 Problem Description

### 1.1 Task 3.2.1

Produce a reliable and validated thermal management simulation tool that can be used in the initial stages of design to correctly evaluate and mitigate the adverse effects of increased heat loads. The seeds of this project lie in previous ESRDC work that resulted in the initial development of two complementary software tools: the Cooling System Design Tool (CSDT), developed by MIT [1], and vemESRDC, developed by FSU. Continued development will merge these tools into a cohesive whole and expand the capabilities, allowing the user to design a cooling system using the state-of-the-art methods to study the impact of design decisions at the early stages of design and allow flexibility to evaluate new equipment or new technologies. This cohesive design tool will be validated using both higher-level modeling tools and experimental data from physical cooling loops systems for operating equipment.

## 2 Summary of Accomplishments

Here are the list of accomplishments at MIT during the year of 2013-2014.

1. We developed and implemented one dimensional time-dependent partial differential equations from first principles to model hydrodynamics and heat transfer in cooling piping networks. Besides the steady-state response of the system, the model can compute the propagation of time-varying operating conditions throughout the cooling system. For instance, the model is capable of quantifying the impact of failure of different components such as chillers, pumps, valves, etc. on the overall cooling system performance. The computational model is fast-to-evaluate, making it suitable for being utilized at early design stages.
2. The computational model was verified with several benchmark problems.
3. In a collaborative effort with Florida State University (FSU), the 1D model was combined with vem-ESRDC to form a single computational tool in which the interaction between the cooling network and the heat loads is modeled. In this two-way coupling, the 1D model simulates the coolant flow and temperature distribution in the network by acquiring the dynamic heat load from vem-ESRDC. On the other hand, vem-ESRDC imports the coolant water temperature and massflow rate from the 1D simulation. The implementation for this task took place while Sam Yang from FSU visited MIT from June to August 2014.

### 3 Task 3.2.1 System-Level Thermal Modeling

#### 3.1 Development of 1D Transient Flow Model (MIT)

##### 3.1.1 Modeling Assumptions

One dimensional models of flow in elastic pipes are derived by reducing the dimensionality of the full Navier-Stokes equations under the following assumptions:

1. Quasi one-dimensional flow: this assumption assumes that the tangential and radial velocity components are zero, *i.e.*  $u_r(r, \theta, x, t) = u_\theta(r, \theta, x, t) = 0$ , adopting a cylindrical coordinate system. As a result of this assumption, using full Navier-Stokes equation one can show that  $\frac{\partial p}{\partial r} = \frac{\partial p}{\partial \theta} = 0$ .
2. Axial symmetry: this assumes that any quantity such as  $u(r, \theta, x, t)$  is independent of the angular location  $\theta$ , and therefore  $u := u(r, x, t)$ . This assumption becomes more accurate if the local curvature of the pipe becomes smaller. For instance, in cases where flow undergoes a sharp turn, such as a 90° or a junction, the axial symmetry may not be a valid assumption. In those cases, we model the component (*i.e.* bend, junction, ...) separately.
3. Fixed radial dependence: the axial velocity profile is assumed to be in the form of

$$u_x(r, x, t) = u(x, t)g(r)$$

where  $u(x, t)$  is the mean of the profile and thus  $\int_0^{r_i} \pi g(r) r dr = \pi r_i^2$ , where  $r_i$  is the internal radius of the pipe. The choices for radial dependence functions depend on the flow direction. For instance, Poiseuille flow profile may be assumed for a laminar flow condition, or an experimental profile may be considered for a turbulent flow condition. As it will be demonstrated later in the report, the explicit profile of  $g(r)$  does not appear in the mathematical modeling. However  $g(r)$  directly affects the friction factor as different choices of  $g(r)$  determines the shear stress at the pipe wall.

##### 3.1.2 Mathematical Modeling

To model the propagation of transient flow in pipes, both the compressibility of the liquid and the elasticity of the pipe must be modeled. Local increase in fluid pressure results in local enlargement of the pipe cross section area. In general unknown variables exist: pressure  $p(x, t)$ , axial velocity  $u(x, t)$  and the cross sectional area  $A(x, t)$ . A purely elastic model provides a pressure-area relation. The Laplace's law provides such a relation:

$$p = p_{ext} + \beta(\sqrt{A} - \sqrt{A_0}), \quad (1)$$

where

$$\beta = \frac{2\rho c^2}{\sqrt{A}}$$

with

$$c^2 = \frac{\frac{K}{\rho}}{1 + (\frac{K}{E})(\frac{D}{e})}.$$

In the above equation,  $c$  is the speed of an acoustical wave through the pipe,  $e$  is the wall thickness of the pipe,  $K$  is the bulk modulus of elasticity of the fluid, and  $E$  is the Young's modulus of the elasticity for the wall material. In order to close the system, two other equations are required, which are provided by conservation of mass and momentum equations:

$$\frac{\partial A}{\partial t} + \frac{\partial uA}{\partial x} = 0 \quad (2)$$

$$\frac{\partial u}{\partial t} + \frac{\partial u^2/2}{\partial x} = -\frac{1}{\rho} \frac{\partial p}{\partial x} - \frac{fu^2}{2D} - g \sin \theta \quad (3)$$

In the above equations,  $f$  is the friction factor in the pipe and it depends on the state of the flow (*i.e.* laminar or turbulent), and the roughness of the pipe wall. The variable  $\theta$  is the angle between the pipe axis and the horizon.

## 3.2 Development of 1D Transient Heat Transfer Model (MIT)

### 3.2.1 Modeling Assumptions

In general temperature is a scalar function in the form of  $T := T(r, \theta, x, t)$  in the pipe network system. Analogous assumptions to the ones used for hydrodynamics are applied to temperature. Namely:

1. Axial symmetry: this assumption relaxes the temperature to the form  $T := T(r, x, t)$ .
2. Fixed radial dependence: similar to the velocity, enforcing this assumption results in the temperature profile in the form of  $T := T(x, t)h(r)$  with  $\int_0^{r_i} \pi h(r)r dr = \pi r_i^2$ .
3. Incompressible flow: we assume that the working fluid is incompressible. Therefore, the internal energy  $e$  is expressed as:

$$e = c_p T,$$

where  $c_p$  is the specific heat capacity.

4. Negligible kinetic energy: the kinetic energy is neglected as it has significantly smaller values compared to the internal energy of liquids such as water. Thus  $e + u^2/2 \simeq e$ .
5. Negligible axial conduction: In most realistic cases, the axial conduction is negligible to the advection terms. Since our physical model has the capability of including axial conduction, throughout the derivation the axial conduction is considered.

### 3.2.2 Mathematical Modeling

Following our assumptions, we consider the control volume as shown in figure 1. The control volume expands to the pipe wall boundary, where energy is exchanged through conduction. Moreover energy crosses the boundary of the control volume by means of axial conduction and advection. The balance of energy for a generic control volume can be written as:

$$\frac{\partial}{\partial t} \oint_V \rho e dV = \oint_S \dot{E}_{adv} dS + \oint_S \dot{E}_{cond} dS \quad (4)$$

The axial advection for the control volume shown in figure 1 is given by:

$$\begin{aligned} \oint_S \dot{E}_{adv} dS &\equiv \dot{E}_{adv,x} - \dot{E}_{adv,x+dx} = \rho u (e + u^2/2) A_x \\ &- \left\{ \rho u (e + u^2/2) A_x + \frac{\partial}{\partial x} [\rho u (e + u^2/2) A_x] dx \right\} \\ &= - \frac{\partial}{\partial x} [\rho u (e + u^2/2) A_x] dx \end{aligned} \quad (5)$$

Using Fourier's law for the heat conduction, the axial conduction is given by:

$$\begin{aligned} \oint_S \dot{E}_{cond} dS &\equiv (\dot{E}_{cond,x} - \dot{E}_{cond,x+dx}) - \dot{E}_{cond,r} = -k \frac{\partial T}{\partial x} A_x \\ &= - \left\{ -k \frac{\partial T}{\partial x} A_x + \frac{\partial}{\partial x} \left[ -k \frac{\partial T}{\partial x} A_x \right] dx \right\} \\ &- q_r'' dA_r \\ &= \frac{\partial}{\partial x} \left[ k \frac{\partial T}{\partial x} A_x \right] dx - q_r'' dA_r \end{aligned} \quad (6)$$

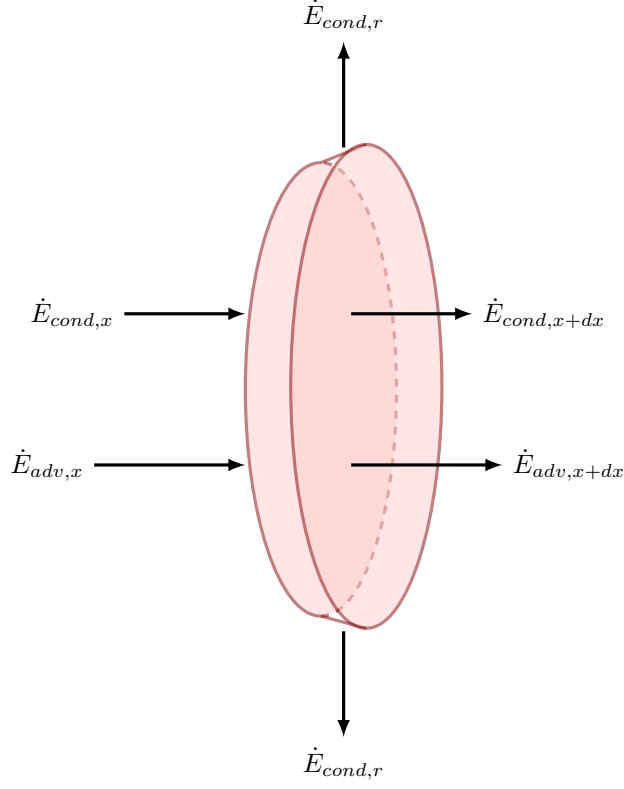


**Figure 1:** Control volume for coolant water for an element inside the pipe.

In the above equation, the radial heat conduction is expressed as:

$$\dot{E}_{cond,r} = q'' dA_r$$

where  $dA_r = 2\pi r_i dx$ . Substituting equations 5 and 6 into equation 4, and after re-arranging results in:

$$\rho c_p \left( \frac{\partial(TA_x)}{\partial t} + \frac{\partial(uTA_x)}{\partial x} \right) = \frac{\partial}{\partial x} \left[ k \frac{\partial T}{\partial x} A_x \right] - 2\pi r_i q_r'' \quad (7)$$

To close the system, the radial heat conduction must be modeled. A cross section of the pipe is shown in figure 2, where the coolant water is shown in blue, pipe wall in gray and pipe insulation in red. Along the heat path from the coolant water to the ambient, shown by subscript  $\infty$ , four thermal resistance exits: (1) the forced convection resistance inside the pipe; (2) the conduction resistance through the pipe wall; (3) the conduction resistance through the pipe insulation and (4) the natural convection resistance with the ambient. The equivalent thermal resistance network is shown in figure 2. As a result, the radial heat conduction can be expressed as:

$$\dot{E}_{cond,r} = q_r'' dA_r = \frac{T - T_\infty}{\frac{1}{2\pi r_i h_i dx} + \frac{\ln(r_p/r_i)}{2\pi k_p dx} + \frac{\ln(r_o/r_p)}{2\pi k_{ins} dx} + \frac{1}{2\pi r_o h_\infty dx}} \quad (8)$$

The above equation can be re-written as:

$$-2\pi r_i q_r'' = \frac{T_\infty - T}{\mathcal{R}_t}, \quad (9)$$

where

$$\mathcal{R}_t = \frac{1}{2\pi r_i h_i} + \frac{\ln(r_p/r_i)}{2\pi k_p} + \frac{\ln(r_o/r_p)}{2\pi k_{ins}} + \frac{1}{2\pi r_o h_\infty} \quad (10)$$

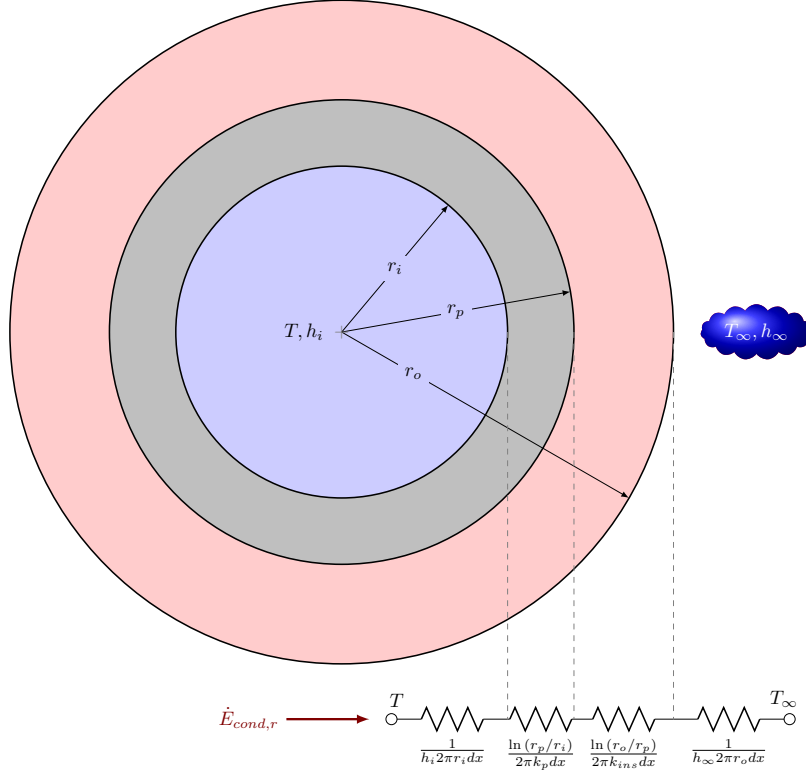


**Figure 2:** Pipe thermal resistance network.

Therefore the energy equation becomes:

$$\rho c_p \left( \frac{\partial \Gamma}{\partial t} + \frac{\partial(u\Gamma)}{\partial x} \right) = \frac{\partial}{\partial x} \left[ k \frac{\partial T}{\partial x} A_x \right] + \frac{T_\infty - T}{\mathcal{R}_t} \quad (11)$$

If the axial conduction is neglected:

$$\rho c_p \left( \frac{\partial \Gamma}{\partial t} + \frac{\partial(u\Gamma)}{\partial x} \right) = \frac{T_\infty - T}{\mathcal{R}_t} \quad (12)$$

The system of partial differential equations for hydrodynamics and heat transfer can be expressed as:

$$\frac{\partial \mathbf{U}}{\partial t} + \mathbf{H} \frac{\partial \mathbf{U}}{\partial x} = \mathbf{F} \quad (13)$$

where:

$$\mathbf{U} = \begin{pmatrix} A \\ u \\ \Gamma \end{pmatrix}, \quad (14)$$

$$\mathbf{H} = \begin{pmatrix} u & A & 0 \\ \frac{1}{\rho D A} & u & 0 \\ 0 & \Gamma & u \end{pmatrix} \quad (15)$$

and

$$\mathbf{F} = \begin{pmatrix} 0 \\ -\frac{1}{\rho} \frac{\partial p}{\partial x} - \frac{f u^2}{2D} - g \sin \theta \\ \frac{\partial}{\partial x} \left[ k \frac{\partial T}{\partial x} A_x \right] + \frac{T_\infty - T}{\mathcal{R}_t} \end{pmatrix}, \quad (16)$$



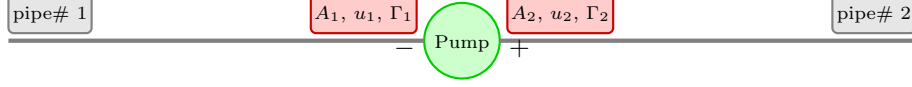


**Figure 3:** The schematic of the pump model.

Given that  $A > 0$ , the matrix  $\mathbf{H}$  has three real eigen-values. Thus the above system can be diagonalized to the following form:

$$\frac{\partial \mathbf{W}}{\partial t} + \mathbf{\Lambda} \frac{\partial \mathbf{W}}{\partial x} = \mathbf{S} \quad (17)$$

where:

$$\mathbf{W} = \begin{pmatrix} W_1 \\ W_2 \\ W_3 \end{pmatrix},$$

with  $W_1$ ,  $W_2$  and  $W_3$  being the Riemann invariants given by:

$$W_1(\mathbf{H}) = u + 4(c - c_0) = u + 4\sqrt{\frac{\beta}{2\rho}}(A^{1/4} - A_0^{1/4}) \quad (18)$$

$$W_2(\mathbf{H}) = u - 4(c - c_0) = u - 4\sqrt{\frac{\beta}{2\rho}}(A^{1/4} - A_0^{1/4}) \quad (19)$$

$$W_3(\mathbf{H}) = \Gamma/A \quad (20)$$

$$(21)$$

and  $\mathbf{\Lambda}$  is diagonal matrix whose entries are:

$$\lambda_1(\mathbf{H}) = u + c; \quad \lambda_2(\mathbf{H}) = u - c; \quad \lambda_3(\mathbf{H}) = u. \quad (22)$$

In most piping network system,  $c \gg u$ , and therefore  $u + c > 0$  and  $u - c < 0$ . As a result the characteristic curve that is obtained from  $dx/dt = u + c$  is *forward traveling* and the characteristic curve with  $dx/dt = u - c$  is *backward traveling*. The characteristic curve obtained by  $dx/dt = u$  can be either forward traveling or backward traveling depending on the sign of  $u$ .

### 3.3 Component Modeling

#### 3.3.1 Pump

A pump is modeled as a zero-dimensional component that connects two pipes, as shown in figure 3. The six unknowns are shown in red. These variables are  $A_1$ ,  $u_1$  and  $\Gamma_1$  from pipe #1 on the suction side of the pump, and  $A_2$ ,  $u_2$  and  $\Gamma_2$  from pipe #2 on the pressure side of the pump. Hydrodynamic variables are independent of temperature and therefore they can be solved independently of temperature. Forward traveling characteristic waves bring information to the pump in pipe # 1, and traveling characteristic waves bring information to the pump in pipe # 2. These two Riemann invariants provide two independent equations. Conservation of mass provides the third equation. The fourth equation is obtained by incorporating the pump characteristic curve, that results in a pressure jump for fluid traveling from pipe #1 to pipe #2. The pressure jump is dependent on the massflow rate passing through the pump. In summary

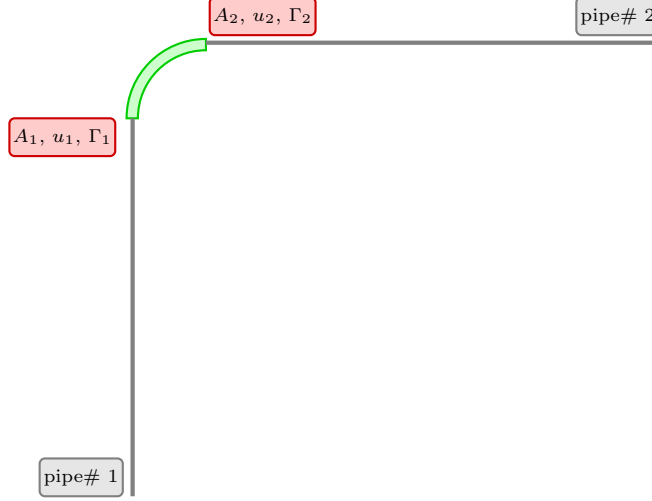


**Figure 4:** The schematic of the bend model.

these four equations are:

$$u_1 + 4\sqrt{\frac{\beta}{2\rho}}(A_1^{1/4} - A_0^{1/4}) = W_1 \quad (23)$$

$$u_2 - 4\sqrt{\frac{\beta}{2\rho}}(A_2^{1/4} - A_0^{1/4}) = W_2 \quad (24)$$

$$A_1 u_1 = A_2 u_2 \quad (25)$$

$$(P_2 + \frac{1}{2}u_2^2) - (P_1 + \frac{1}{2}u_1^2) = P_p(A_1 u_1) \quad (26)$$

Note that the pressure is algebraically related to area through the constitutive model given by equation 1. The above four equations form a nonlinear system of equations that are solved at every time step using Newton-Raphson method.

We assume that the pump is an adiabatic component, thus balance of energy requires:

$$u_1 \Gamma_1 = u_2 \Gamma_2. \quad (27)$$

After considering conservation of mass the above equation becomes:

$$T_1 = T_2. \quad (28)$$

The other equation is provided by information ( $W_3$ ) propagated along the characteristic line. The characteristic can be forward or backward traveling depending on the sign of  $u_1$  ( $u_2$  has the same sign). Therefore:

$$\begin{aligned} \text{if } u \geq 0, \quad T_1 &= W_3 \\ \text{if } u < 0, \quad T_2 &= W_3 \end{aligned}$$

### 3.3.2 Bend

Similar to the pump, six unknowns exist that have to be solved for by modeling the bend. Bend is modeled as a zero-dimensional component by considering pressure loss as the fluid passes through the bend. The pressure loss can be modeled as:

$$\Delta p_{loss} = K_{L,bend} \frac{1}{2} \rho u_1^2$$



**Figure 5:** The schematic of the valve model.

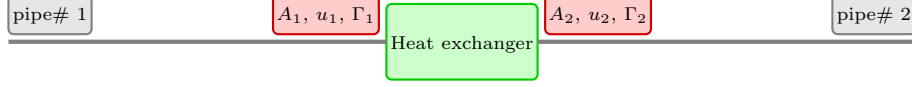


**Figure 6:** The schematic of the heat exchanger model.

where  $K_{L,bend} = \phi(\text{geometry}, Re)$ . Thus the hydrodynamic variables can be found using:

$$u_1 + 4\sqrt{\frac{\beta}{2\rho}}(A_1^{1/4} - A_0^{1/4}) = W_1 \quad (29)$$

$$u_2 - 4\sqrt{\frac{\beta}{2\rho}}(A_2^{1/4} - A_0^{1/4}) = W_2 \quad (30)$$

$$A_1 u_1 = A_2 u_2 \quad (31)$$

$$P_2 - P_1 = \frac{1}{2} K_{L,bend} u_1^2 \quad (32)$$

The temperature is modeled in an identical fashion as that of the pump model, since bend is assume to be an adiabatic component.

### 3.3.3 Valve

Valve modeled is analogous to that of the bend, with the only difference on the nature of the pressure loss. The schematic is shown in figure 5. The pressure loss through the valve depends on valve opening and Reynolds number. Thus  $K_{L,valve} = \phi(\text{valve opening}, Re)$ .

$$u_1 + 4\sqrt{\frac{\beta}{2\rho}}(A_1^{1/4} - A_0^{1/4}) = W_1 \quad (33)$$

$$u_2 - 4\sqrt{\frac{\beta}{2\rho}}(A_2^{1/4} - A_0^{1/4}) = W_2 \quad (34)$$

$$A_1 u_1 = A_2 u_2 \quad (35)$$

$$P_2 - P_1 = \frac{1}{2} K_{L,valve} u_1^2 \quad (36)$$

### 3.3.4 Heat Exchanger

The schematic of heat exchanger model is shown in figure 6. The hydrodynamic model for a heat exchanger is similar to bend or valve, since we model the heat exchanger as zero-dimensional component with friction pressure losses for the fluid as it passes through the heat exchanger. Therefore:

$$\Delta p_{loss} = K_{L,hx} \frac{1}{2} \rho u_1^2$$

where  $K_{L,hx} = \phi(\text{heat exchanger type}, Re)$ . As a result the four unknown  $A_1, u_1, A_2$  and  $u_2$  can

be computed by solving the system following system of nonlinear equations:

$$u_1 + 4\sqrt{\frac{\beta}{2\rho}}(A_1^{1/4} - A_0^{1/4}) = W_1 \quad (37)$$

$$u_2 - 4\sqrt{\frac{\beta}{2\rho}}(A_2^{1/4} - A_0^{1/4}) = W_2 \quad (38)$$

$$A_1 u_1 = A_2 u_2 \quad (39)$$

$$P_2 - P_1 = \frac{1}{2} K_{L,hx} u_1^2 \quad (40)$$

To compute  $\Gamma_1$  and  $\Gamma_2$  we use the balance of energy for the coolant fluid. This follows:

$$\dot{Q} = \dot{m} c_p (T_2 - T_1)$$

In this setting,  $\dot{Q}$  is the amount of heat absorbed from the heat load. The value of  $\dot{Q}$  depends on the temperature difference between the coolant and the component that is being cooled, the massflow rate of the coolant, and the type of heat exchanger. The value of  $\dot{Q}$  is obtained by coupling the 1D model to vem-ESRDC, as it is explained in the next section.

Substituting for  $\dot{m} = \rho u_1 A_1 = \rho u_2 A_2$  and the definitions of  $\Gamma_1 = T_1 A_1$  and  $\Gamma_2 = T_2 A_2$ , we arrive at:

$$\dot{Q} = \rho c_p (u_2 \Gamma_2 - u_1 \Gamma_1)$$

To close the system, we use the information that propagates along the characteristic  $dx/dt = u$ . This follows:

$$\begin{aligned} \text{if } u &\geq 0, & T_1 &= W_3 \\ \text{if } u &< 0, & T_2 &= W_3. \end{aligned}$$

### 3.4 Numerical Method

A brief outline of the numerical method introduced in [2] is presented here. For more details on the numerical method see [3]. The system of equation solved is:

$$\frac{\partial \mathbf{U}}{\partial t} + \frac{\partial \mathbf{F}(\mathbf{U})}{\partial x} = \mathbf{S}(\mathbf{U}) \quad (41)$$

where

$$\mathbf{U} = \begin{bmatrix} U_1 \\ U_2 \end{bmatrix} = \begin{bmatrix} A \\ u \end{bmatrix}, \quad \mathbf{F} = \begin{bmatrix} F_1 \\ F_2 \end{bmatrix} = \begin{bmatrix} uA \\ \frac{u^2}{2} + \frac{p}{\rho} \end{bmatrix}, \quad \mathbf{S} = \begin{bmatrix} S_1 \\ S_2 \end{bmatrix} = \begin{bmatrix} 0 \\ -\frac{uf}{A} \end{bmatrix}$$

The computational domain  $\Omega$  consists of arterial segments, which can be divided in  $N_{el}$  elemental non-overlapping regions  $\Omega_e = (x_e^L, x_e^R)$ , such that  $x_e^R = x_{e+1}^L$  for  $e = 1, \dots, N_{el}$ . The discontinuous Galerkin formulation requires, for each element  $e = 1, \dots, N_{el}$ , the resolution of the system:

$$J_e \frac{\partial \hat{U}_{i,e}^p}{\partial t} = -J_e \int_{\Omega_e} L_p \frac{\partial F_i}{\partial x} d\xi - L_p [F_i^u - F_i]_{x_e^L}^{x_e^R} + J_e \int_{\Omega_e} L_p S_i d\xi, \quad p = 0, \dots, P, \quad i = 1, 2, \quad (42)$$

where  $\mathbf{U}$  has been discretized by  $\mathbf{U}^\delta$  written in terms of orthonormal Legendre polynomials  $L_p(x)$ :

$$\mathbf{U}^\delta|_{\Omega_e} = \sum_{p=0}^P L_p \hat{\mathbf{U}}_e^p$$

Each element is mapped onto a reference element  $\Omega_{st} = \{-1 \leq \xi \leq 1\}$  called the "standard element" and  $J_e$  is the Jacobian of the corresponding affine mapping:

$$J_e = \frac{1}{2}(x_e^R - x_e^L), \quad x_e(\xi) = x_e^L \frac{(1 - \xi)}{2} + x_e^R \frac{(1 + \xi)}{2}$$

$\mathbf{F}^u$  is the upwinded flux that propagates information between the elemental regions and the bifurcations of the system. At the inlet and outlet boundary elements, the fluxes are upwinded by means of the boundary conditions. The hyperbolicity of the system requires one boundary condition at each terminal end.

An Adams-Bashforth scheme is used for the time integration:

$$\frac{\partial \hat{U}_{i,e}^p}{\partial t} = f(\hat{U}_{i,e}^p)$$

with,

$$(\hat{U}_{i,e}^p) = - \int_{\Omega_e} L_p \frac{\partial F_i}{\partial x} d\xi - \frac{1}{J_e} L_p [F_i^u - F_i]_{x_e^L}^{x_e^R} + \int_{\Omega_e} L_p S_i d\xi,$$

then,

$$(\hat{U}_{i,e}^p)^{n+1} = (\hat{U}_{i,e}^p)^n + \frac{3\Delta t}{2} f((\hat{U}_{i,e}^p)^n) - \frac{\Delta t}{2} f((\hat{U}_{i,e}^p)^{n-1})$$

### 3.5 Coupling of $\mathcal{N}\epsilon\kappa\tau\alpha r1d$ and vemESRDC: Collaboration between MIT and FSU

In the current strategy, vemESRDC and  $\mathcal{N}\epsilon\kappa\tau\alpha r1d$  perform a "hand-shake" at every time step. If the steady-state solution is sought, the time-steps perform the role of the iterations to reach the steady-state solution. The algorithm of the coupling between the two codes is shown in figure 8. **vemESRDC:**

In vemESRDC, the transient balance of energy is solved, with the difference of the heat exchanger absorbing part of the heat load. In fact, heat exchanger and the surrounding elements, through convection or conduction or both, compete to absorb the heat load. The net amount of heat left in the right hand side of the equation 43 will decrease or increase the element temperature  $T_i$ . In equation 43:

- The inlet temperature of cooling water,  $T_{cw,in}$ , is provided to vemESRDC by  $\mathcal{N}\epsilon\kappa\tau\alpha r1d$ , and is a known quantity at each time-step.
- The heat load  $\dot{Q}_{gen}$  is known and is provided by LEAPS.
- The interaction of temperature at element  $T_i$  with neighbor elements is done through convection or conduction or the combination of the two, which forms a system of unknowns already implemented at vemESRDC. For more details see [4].

$$\frac{dT_i}{dt} = \frac{1}{\rho_i V_i c_i} \left( U_{HX} A_{HX} (T_{cw,in} - T_i) + \dot{Q}_{gen} + \sum_{j=E,W,S,N,T,B} Q_j \right). \quad (43)$$

$\mathcal{N}\epsilon\kappa\tau\alpha r1d$ :

The calculation and book-keeping of cooling water (fresh water, sea water, ...) temperatures are done in  $\mathcal{N}\epsilon\kappa\tau\alpha r1d$ . Once the solution of vemESRDC is obtained at each time-step,  $T_i$ 's for all elements are obtained and a balance of energy, for the heat exchanger is used to calculate the cooling water outlet temperature from the heat exchanger. The balance of energy for the heat exchanger requires:

$$U_{HX} A_{HX} (T_i - T_{cw,in}) = \dot{m}_{cw} c_{cw} (T_{cw,out} - T_{cw,in}) \quad (44)$$

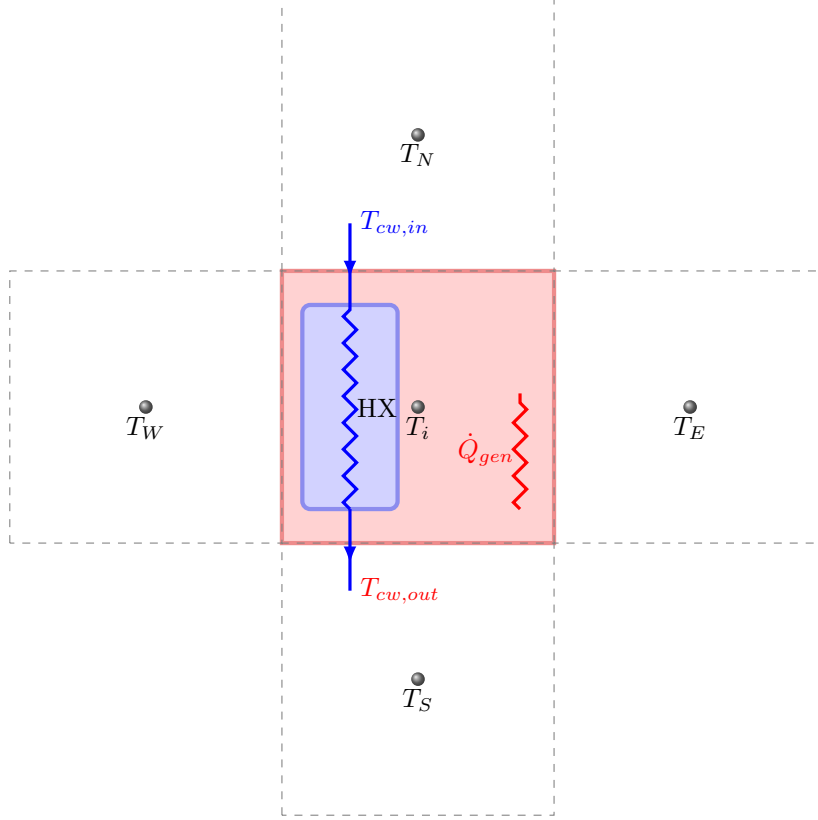


**Figure 7:** A 2D schematic of element-equipment arrangement of thermal systems in All-Electric-Ships. The three-dimensional version is only the extension of the above sketch by having a top (T) and bottom (B) elements in the perpendicular view. In the above the following identifiers are used: HX: Heat Exchanger; CW: Cooling Water;  $\dot{Q}_{gen}$ : the heat load at the volume element  $i$ ; E: East; W: West; N: North; S: South.

From the above equation,  $T_{cw,out}$  can be calculated:

$$T_{cw,out} = \frac{1}{\dot{m}_{cw}c_{cw}} U_{HX} A_{HX} (T_i - T_{cw,in}) + T_{cw,in} \quad (45)$$

The massflow rate in the cooling water network,  $\dot{m}_{cw}$ , is also calculated by  $\mathcal{N}\epsilon\kappa\tau\alpha r1d$  by solving transient quasi one-dimensional Navier-Stokes equations.

**Note:**

In cases where the heat exchanger interaction with the heat load, not only requires  $T_{cw,in}$ , but it also requires the cooling outlet temperature  $T_{cw,out}$ , at each time-step, iterations between vemESRDC and  $\mathcal{N}\epsilon\kappa\tau\alpha r1d$  have to be performed.

### 3.6 Verification and Validation (MIT)

#### 3.6.1 A Single Loop with a Pump

As a first verification example, we consider a single pipe loop as shown in figure 9. The fluid is driven by a single pump. The fluid is considered to be sea water with the properties given in table 1.

The pipe is chosen from ANSI Schedule 80, a steel pipe with 1" diameter and the thickness of 1/8". The pipe characteristics are given in table 2. The characteristic curve of the pump is

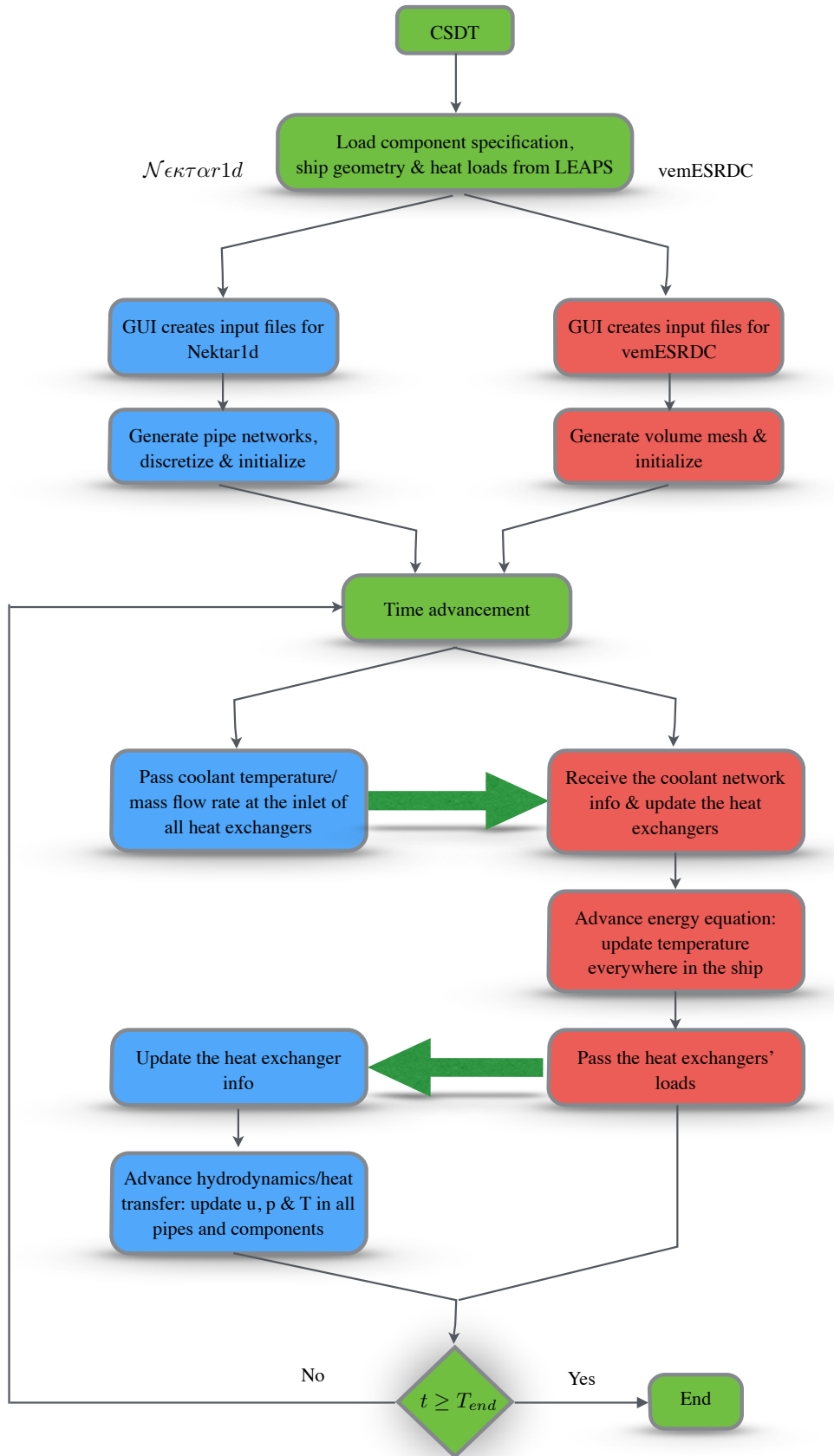


**Figure 8:** The algorithm for coupling *Nektar1d* and vem-ESRDC into a single computational tool.

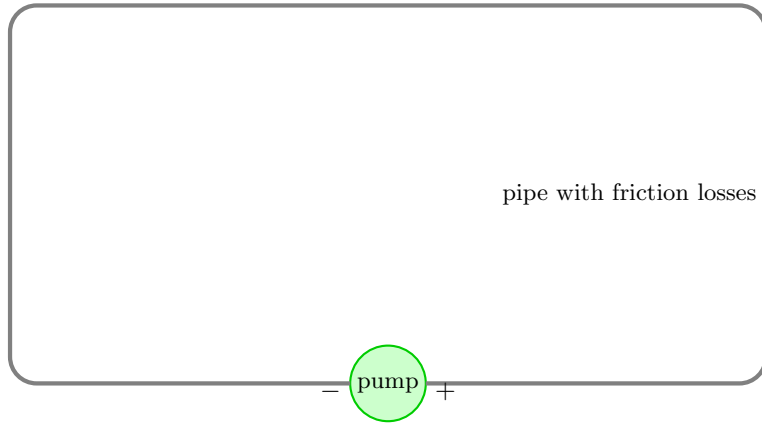


**Figure 9:** The schematic of the verification problem: a single loop driven by a pump.

**Table 1:** Sea water physical properties for verification problem.

Density ( $Kg/m^3$ )	Bulk modulus of elasticity (Pa)	Dynamic viscosity (Pa s)
$1.028 \times 10^3$	$2.39 \times 10^9$	$1.88 \times 10^{-3}$

**Table 2:** Pipe properties for verification problem.

Length (m)	Diameter (inch)	Wall thickness (inch)	Young's modulus (Pa)
100	1"	1/8"	$1.84 \times 10^{11}$



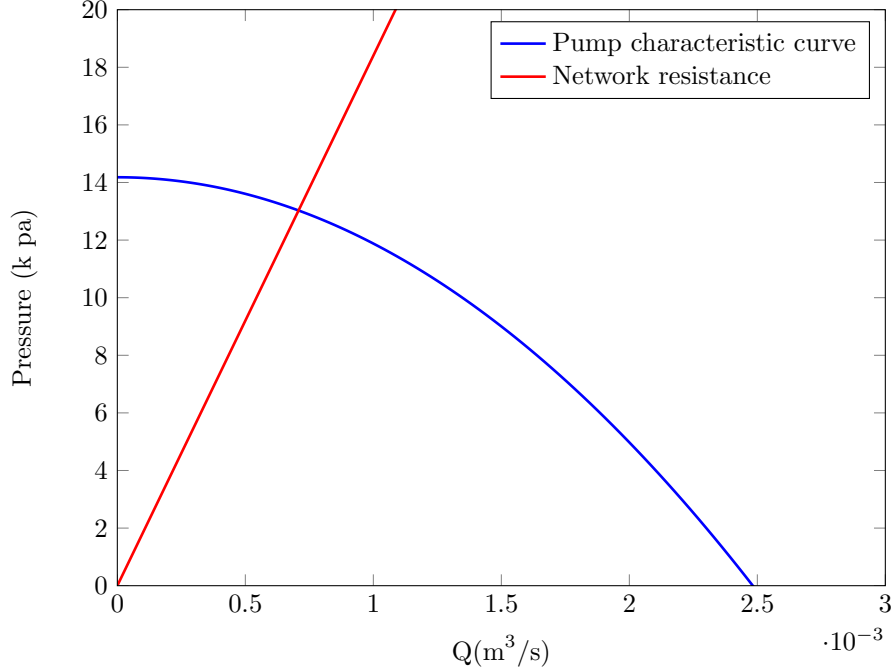


**Figure 10:** Pump characteristic curve and network resistance. The intersection of the two curve shows the steady state operating point of the pump/network.

assumed to be given by a polynomial-fitted curve given below:

$$P_{pump}(Q) = a - bQ^2,$$

with

$$a = 1.42 \times 10^4, \quad b = 2.30 \times 10^9,$$

where  $Q$  is the volumetric flowrate in  $m^3/s$ , and  $P$  is the pressure increase across the pump in Pa. We assume the flow in the pipe remains laminar and thus the friction factor can be obtained analytically:

$$f = \frac{64}{Re}.$$

The network resistance curve is obtained by computing the friction loss versus different volumetric flowrates. Thus:

$$P_{res}(Q) = \frac{fL}{D} \frac{\rho Q^2}{2A^2}$$

After replacing the friction coefficient in the above equation, the resistance pressure versus volumetric mass flowrate can be obtained:

$$P_{res}(Q) = \frac{8\pi\mu QL}{A^2}$$

In figure 10, the pump characteristic curve and the network resistance are shown. The exact steady-state solution is obtained by finding the intersection of the pump characteristics curve and the pipe resistance. Therefore the steady-state point can be obtained by:

$$P_{res}(Q_{ss}) = P_{pump}(Q_{ss}).$$

For the given parameters, the operating steady-state volumetric flowrate and pressure for the pump become:

$$Q_{ss} = 7.079 \times 10^{-1} \text{ Liter/sec}; \quad P_{ss} = 13.028 \text{ K Pa.}$$

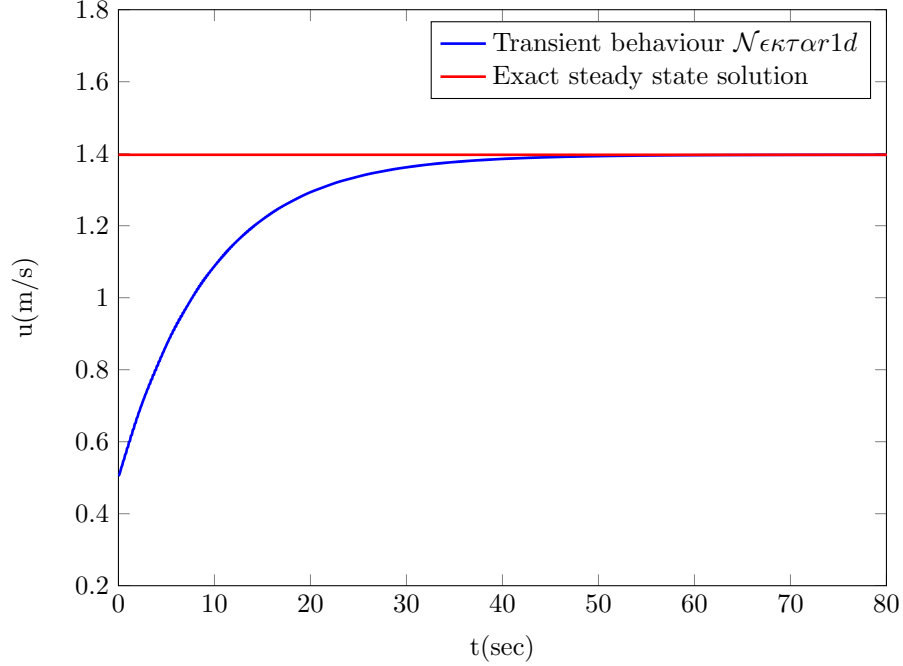


**Figure 11:** The transient behavior of the axial velocity  $u(x, t)$  for single-loop network. The axial velocity exponentially converges to the exact steady state variable.

Given that the pipe diameter is unchanged, the steady-state velocity is constant every in the pipe and thus:

$$u_{ss}(x) = \frac{Q_{ss}}{A} = 1.397\text{m/sec.}$$

In figure 11 the evolution of axial velocity is shown. The axial velocity converges exponentially to the steady state value. Since the pipe area variation during the transient period is very small, conservation mass of requires that  $\frac{\partial u}{\partial x} \simeq 0$ . Therefore transient axial velocity in the pipe is independent of  $x$ .

Since the velocity is constant along the pipe, the pressure gradient along the pipe is constant ( $dp/dx = c$ ). Therefore pressure varies linearly along the pipe according to:

$$p_{ss}(x) = p_{ref} - \frac{8\pi\mu Qx}{A^2}.$$

Figure 12 shows the comparison of the steady state pressure calculated by  $\mathcal{N}\epsilon\kappa\tau\alpha r1d$  along with the exact solution. An excellent match is observed.

### 3.6.2 $\mathcal{N}\epsilon\kappa\tau\alpha r1d$ -vemESRDC Coupling (MIT-FSU)

To verify the strategy and the implementation of the coupling of  $\mathcal{N}\epsilon\kappa\tau\alpha r1d$  and vem-ESRDC, we consider a nine-element volume discretization. The 2D schematic of the volume elements is shown in figure 13.

All elements have equal size with  $\Delta x = \Delta y = \Delta z = 1$ . The volume has adiabatic boundary condition on all its surrounding faces. The middle element (element No. 5) has a time-varying heat load as given by:

$$Q_{gen}(t) = Q(\sqrt{a_1^2 + a_2^2 + a_3^2} - a_1 \sin(\omega_1 t - \phi_1) - a_2 \sin(\omega_2 t - \phi_2) - a_3 \sin(\omega_3 t - \phi_3))$$

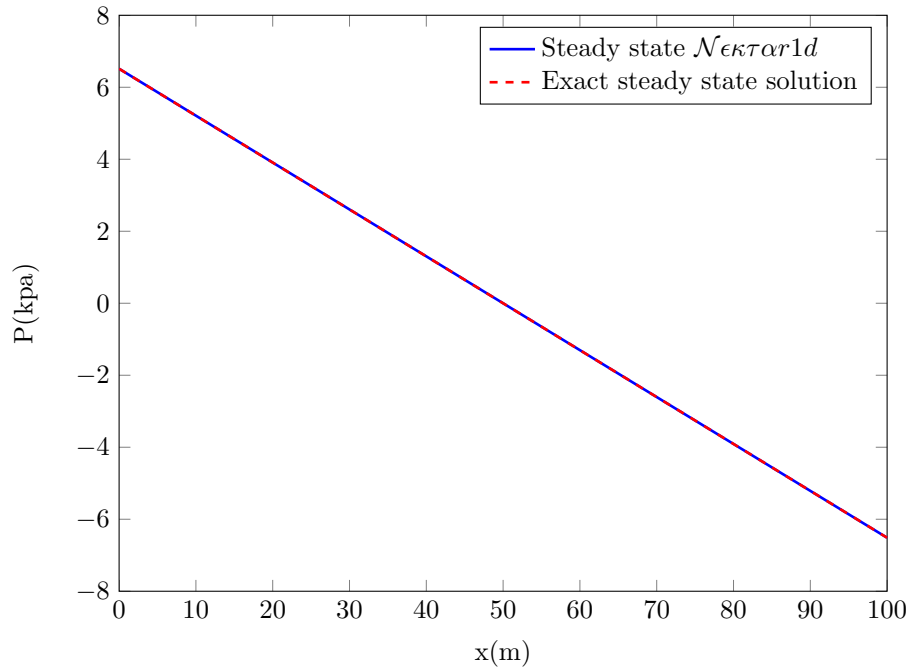


**Figure 12:** Comparison of the steady state pressure obtained from the one dimensional model with exact solution.

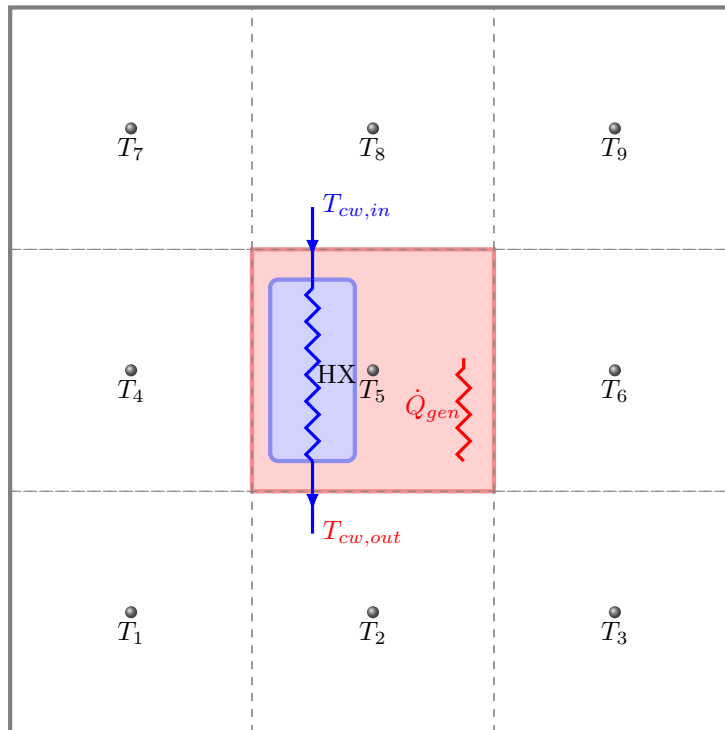


**Figure 13:** The 2D schematic of volume discretization for vem-ESRDC.

**Table 3:** Material properties of solid volume elements for vem-ESRDC calculations.

Density ( $Kg/m^3$ )	Specific heat capacity ( $J/Kg \cdot K$ )	Thermal conductivity ( $W/m^2 \cdot K$ )
$7 \times 10^3$	4.5	55

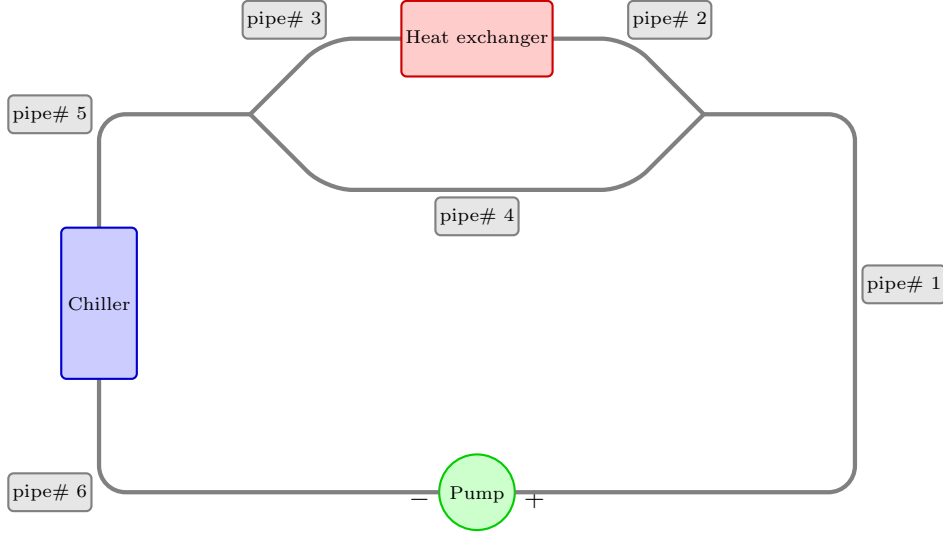


**Figure 14:** The schematic of pipe network configuration for  $\mathcal{N}_{\epsilon\kappa\tau\alpha r1d}$ -vemESRDC Coupling.

$$\begin{aligned}
 Q &= 5000W \\
 a_1 &= 1, a_2 = 0.5, a_3 = 0.1 \\
 \omega_1 &= 0.1, \omega_2 = 0.3, \omega_3 = 0.5(1/sec) \\
 \phi_1 &= 0, \phi_2 = \pi/4, \phi_3 = \pi/8
 \end{aligned}$$

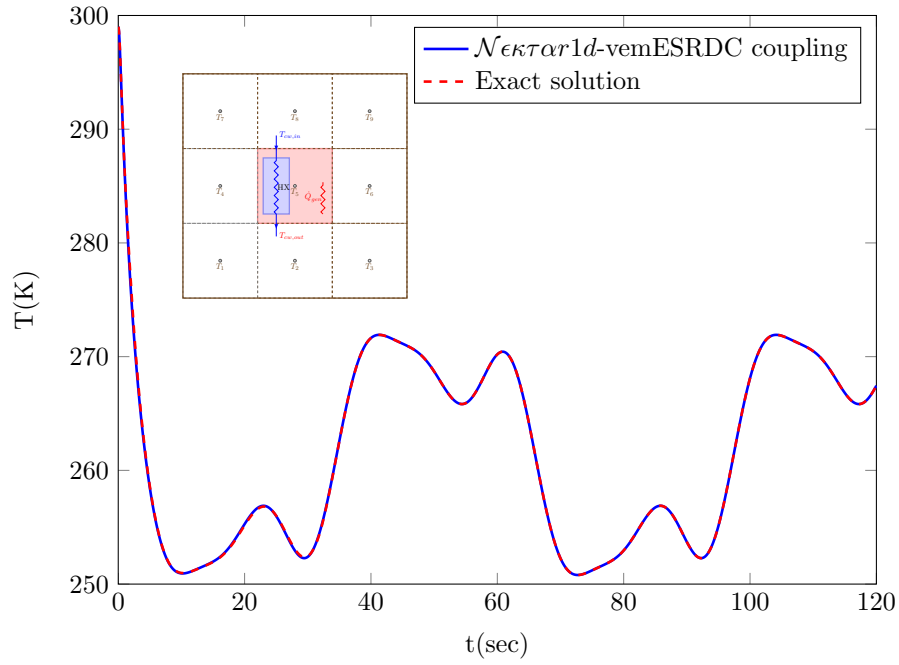
All the elements have the same material property as shown in table 3. Elements are assumed to be solid and therefore they exchange heat with their neighbor elements merely through conduction. The element No. 5 exchanges heat with a heat exchanger, connected to a cooling water network. The cooling water network is shown in figure 14. The cooling network is comprised of six pipes with dimensions given in table 4, and a pipe with the same specification as that of in the previous verification case with characteristic curve shown in figure 10. the heat exchanger is assumed to have a constant heat transfer coefficient with

$$U_{HX}A_{HX} = 500W/K.$$

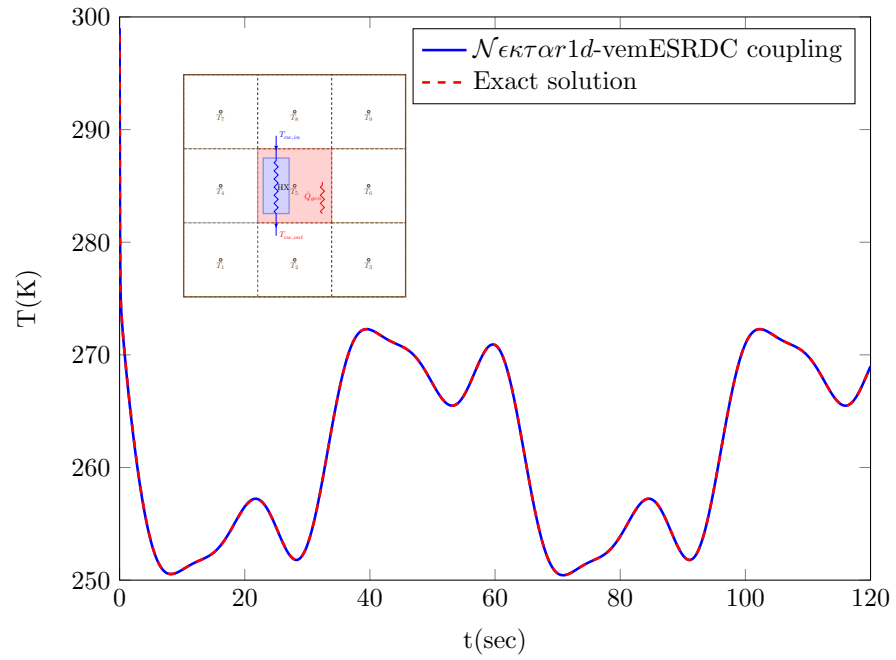
The second heat exchanger is a chiller with time varying heat absorption capacity. The chiller is assume to operate such that the temperature of the coolant water leaving the chiller is set to be  $T_{chiller,out} = 250K$ . All pipes are assumed to have perfect insulations where  $k_{ins} \simeq 0$  and thus  $\mathcal{R}_t \rightarrow \infty$ . We also assume that the axial heat conduction is neglected. The initial temperature in all pipes is assumed to be  $T = 250K$ . The coolant is assumed to be water. The initial velocity in all pipes is assumed to have the steady state values to avoid initial transient behavior.

**Table 4:** Pipe properties used for the verification of  $\mathcal{N}\epsilon\kappa\tau\alpha r1d$ -vemESRDC coupling.

Pipe number	Length (m)	Diameter (inch)
1	40	1''
2	20	1/8''
3	20	1/8''
4	40	1/8''
5	20	1''
6	20	1''



(a)



(b)

**Figure 15:** Comparison of the time-dependent temperature at volume elements with two-way coupling between  $\mathcal{N}\epsilon\kappa\tau\alpha r1d\text{-vemESRDC}$ : (a) Element No. 1; (b) Element No. 5.

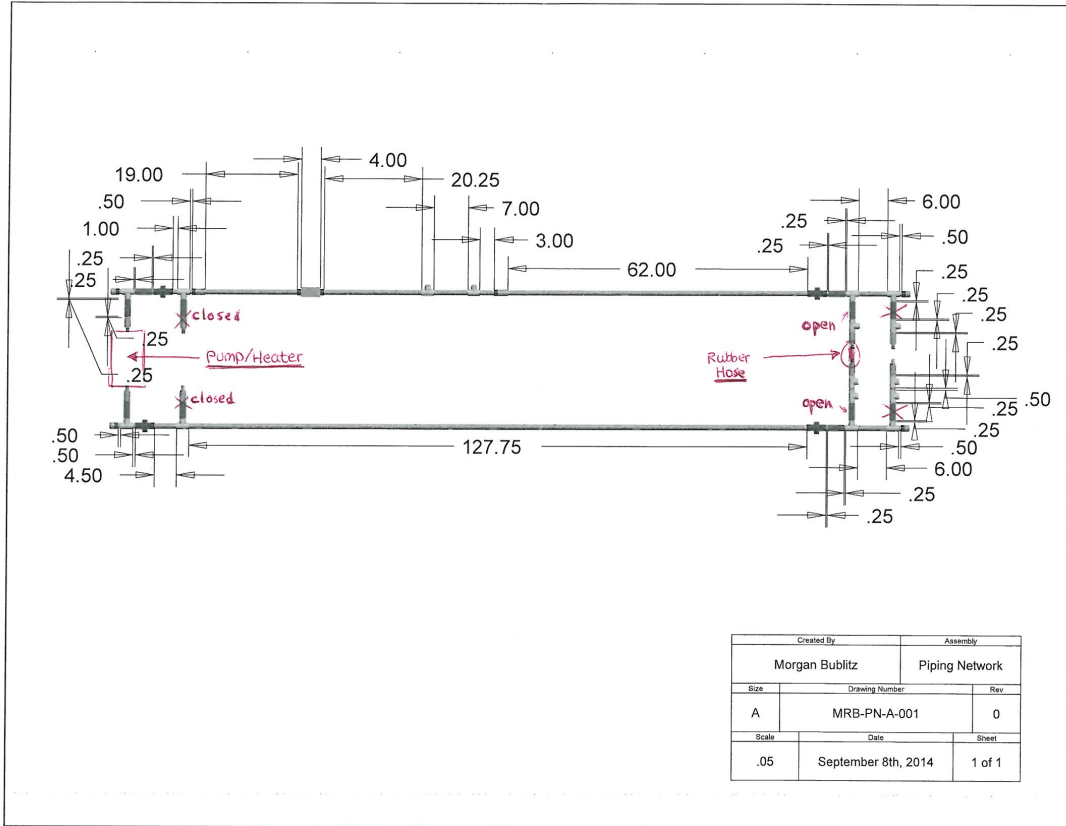


**Figure 16:** Experimental setup of pipe network at Florida State University.

## 4 Conclusion and Future Work

To this end, we have developed and implemented a one-dimensional model for cooling piping networks and their components. We also combined the 1D model with vem-ESRDC in collaboration with Florida State University. In the next year, we will focus on improving the component model, and the experimental validation of our computational tool. More specifically:

1. We will improve the heat exchanger models, taking into account different types of heat exchangers, incorporating higher fidelity reduced order models, and integrating these models with the 1D model.
2. We will improve models for valve, bend and pump by implementing more accurate approximation for loss coefficients in the case of valve and bend. We model scenarios with revers flow in pumps.
3. We will validate our piping and component models with experimental measurements carried out at Florida State University. The drawing of the experimental pipe network built at Florida State University is shown figure 16.
4. We will develop a Graphic User Interface (GUI) that provides an interactive environment for users to use our computational tool.

## References

- [1] Amiel B. Sanfiorenzo. Cooling system design tool for rapid development and analysis of chilled water systems aboard u.s. navy surface ships. Master's thesis, Massachusetts Institute of Technology, 2013.
- [2] S.J. Sherwin, V. Franke, J. Peiro, and K. Parker. One-dimensional modelling of a vascular network in space-time variables. *Journal of Engineering Mathematics*, 47(3-4):217–250, 2003.
- [3] Bernardo Cockburn and Chi-Wang Shu. The runge–kutta discontinuous galerkin method for conservation laws v: Multidimensional systems. *Journal of Computational Physics*, 141(2):199–224, 4 1998.
- [4] Jvc Vargas, Ja Souza, R Hovsopian, Jc Ordonez, T Chiocchio, J Chalfant, C Chryssostomidis, and E Dilay. Notional all-electric ship systems integration thermal simulation and visualization. *Simulation*, 88(9):1116–1128, September 2012.